Cell Calcium 54 (2013) 95–104

Contents lists available at SciVerse ScienceDirect

Cell Calcium

journal homepage: www.elsevier.com/locate/ceca

# Kainate-induced calcium overload of cortical neurons *in vitro*: Dependence on expression of AMPAR GluA2-subunit and down-regulation by subnanomolar ouabain

Polina A. Abushik[a,c], Dmitry A. Sibarov[a,c], Misty J. Eaton[b], Serguei N. Skatchkov[b,**], Sergei M. Antonov[a,c,*]

[a] *Sechenov Institute of Evolutionary Physiology and Biochemistry, Russian Academy of Sciences, Saint-Petersburg, Russian Federation*
[b] *Department of Biochemistry, Universidad Central del Caribe, School of Medicine, Bayamón, PR, USA*
[c] *Laboratory of Molecular Neurodegeneration, Saint-Petersburg State Polytechnical University, Saint-Petersburg, Russian Federation*

ARTICLE INFO

*Article history:*
Received 4 March 2013
Received in revised form 25 April 2013
Accepted 2 May 2013
Available online 28 May 2013

*Keywords:*
Calcium
Excitotoxicity
Cortical neurons
Glutamate receptors
Ouabain
Whole-cell currents
Subunit selective antagonists

ABSTRACT

Whereas kainate (KA)-induced neurodegeneration has been intensively investigated, the contribution of α-amino-3-hydroxy-5-methyl-4-isoxazolepropionic acid receptors (AMPARs) in neuronal $Ca^{2+}$ overload ($[Ca^{2+}]_i$) is still controversial. Using $Ca^{2+}$ imaging and patch-clamp techniques, we found different types of $Ca^{2+}$ entry in cultured rat cortical neurons. The presence of $Ca^{2+}$ in the extracellular solution was required to generate the $[Ca^{2+}]_i$ responses to 30 μM *N*-methyl-D-aspartate (NMDA) or KA. The dynamics of NMDA-induced $[Ca^{2+}]_i$ responses were fast, while KA-induced responses developed slower reaching high $[Ca^{2+}]_i$. Ifenprodil, a specific inhibitor of the GluN2B subunit of NMDARs, reduced NMDA-induced $[Ca^{2+}]_i$ responses suggesting expression of GluN1/GluN2B receptors. Using IEM-1460, a selective blocker of $Ca^{2+}$-permeable GluA2-subunit lacking AMPARs, we found three neuronal responses to KA: (i) IEM-1460 resistant neurons which are similar to pyramidal neurons expressing $Ca^{2+}$-impermeable GluA2-rich AMPARs; (ii) Neurons exhibiting nearly complete block of both KA-induced currents and $[Ca^{2+}]_i$ signals by IEM-1460 may represent interneurons expressing GluA2-lacking AMPARs and (iii) neurons with moderate sensitivity to IEM-1460. Ouabain at 1 nM prevented the neuronal $Ca^{2+}$ overload induced by KA. The data suggest, that cultured rat cortical neurons maintain functional phenotypes of the adult brain cortex, and demonstrate the key contribution of the Na/K-ATPase in neuroprotection against KA excitotoxicity.

© 2013 The Authors. Published by Elsevier Ltd. Open access under CC BY-NC-ND license.

## 1. Introduction

Excessive activation of ionotropic polyamine-sensitive glutamate receptors (GluR) in the vertebrate central nervous system (CNS) [1] induces neurodegeneration, developing via necrosis and apoptosis [2–4], that contributes to the pathogenesis of many neurodegenerative diseases, stroke, motor disorders and spinal cord and brain injuries [5–8]. Excitotoxicity [2,7–9] that results from functional disruption of cellular metabolism is initiated due to non-quantal release of glutamate from neurons and glial cells and its subsequent accumulation in the extracellular space [10–12]. Ionotropic GluRs, especially NMDA (*N*-methyl-D-aspartate, NMDAR) type, whose channels have high conductance to $Ca^{2+}$ [13,14], are generally believed to predominate in triggering excitotoxicity. Application of glutamate or NMDA to primary neuronal cultures causes marked elevations of intracellular free $Ca^{2+}$, because of $Ca^{2+}$ entry from the extracellular medium into neurons through the NMDAR channels [15,16]. This $[Ca^{2+}]_i$ increase is followed by delayed calcium deregulation – a dramatic accumulation of free intracellular $Ca^{2+}$ that reaches micromolar concentrations as a result of mitochondrial dysfunction and $Ca^{2+}$ release from intracellular stores [9,16,17]. Delayed calcium deregulation is thought to trigger the irreversible mechanisms of neuronal death [9].

Though the role of NMDARs in excitotoxicity can hardly be underestimated, there is yet another pathway leading to similar destructive results. NMDARs are strongly blocked by physiological extracellular magnesium, whereas AMPARs can be easily

* Corresponding author at: Sechenov Institute of Evolutionary Physiology and Biochemistry, Russian Academy of Sciences, Torez pr. 44, Saint-Petersburg 194223, Russian Federation.
Tel.: +7 812 5528554; fax: +7 812 5523012.
** Corresponding author at: Department of Biochemistry, Universidad Central del Caribe, School of Medicine, Box 60-327, Bayamón, PR 00960-6032, USA.
Tel.: +1 787 671 7054; fax: +1 787 786 6285.
*E-mail addresses:* serguei.skatchkov@uccaribe.edu, sergueis50@yahoo.com (S.N. Skatchkov), antonov452002@yahoo.com, antonov@iephb.ru (S.M. Antonov).

0143-4160 © 2013 The Authors. Published by Elsevier Ltd. Open access under CC BY-NC-ND license.
http://dx.doi.org/10.1016/j.ceca.2013.05.002

opened [14]. Therefore, other glutamate receptor channels can contribute considerably to the $Ca^{2+}$-entry in response to glutamate. Endogenous glutamate activates α-amino-3-hydroxy-5-methyl-4-isoxazolepropionic acid receptors (AMPARs), whose main function is the generation of fast excitatory synaptic currents (EPSCs) in response to quantal transmitter release from presynaptic terminals [1]. NMDARs generate slower EPSCs than AMPARs. Kainate (KA), a selective nondesensitizing agonist of ionotropic AMPARs [18,19] is also able to trigger neurodegeneration [4,20], similar to NMDA and glutamate. In the case of AMPARs, the intracellular $Ca^{2+}$ signal is determined by expression or withdrawal of the GluA2 subunit of AMPARs which governs $Ca^{2+}$ permeability of their channels [1,14,21]. In the brain, different types of neurons express AMPARs of different subunit content. For example, using the selective open channel blocker IEM-1460, it has been demonstrated that pyramidal neurons isolated from rat hippocampal slices express GluA2-containing AMPARs, whereas interneurons express GluA2-lacking AMPARs or both receptor compositions [22]. Considering this pattern of GluA2 expression one may predict that cultured cortical neurons (also comprised of interneurons and principal cells) should generate differential intracellular $Ca^{2+}$ responses upon activation of their AMPARs. Nevertheless, KA is capable of increasing the frequency of intracellular $Ca^{2+}$ oscillations and promoting $Ca^{2+}$ deregulation in various neuronal types [23,24].

Here we study the dynamics of intracellular $Ca^{2+}$ signals induced by NMDA or KA in primary cultures of rat cortical neurons. Using subunit selective inhibitors such as (i) ifenprodil, a specific blocker of GluN2B of NMDARs [25,26], and (ii) IEM-1460, a selective blocker of $Ca^{2+}$-permeable GluA2-lacking AMPAR channels [22,27], we investigated the subunit compositions of GluRs that are responsible for the $Ca^{2+}$ entry under the conditions of prolonged NMDAR and AMPAR activation. Based upon the degree of IEM-1460 block of intracellular $Ca^{2+}$ responses and currents induced by KA, we distinguished three receptor expression phenotypes displayed by cortical neurons in primary cultures. They correspond to principal neurons expressing GluA2-containing AMPARs, interneurons expressing GluA2-lacking AMPARs and interneurons that express both compositions of AMPARs. Ouabain at 1 nM prevented the $Ca^{2+}$ overload caused by KA, revealing the contribution and the key role of Na/K-ATPase in regulation of intracellular $Ca^{2+}$ homeostasis.

## 2. Materials and methods

### 2.1. Animals

All procedures using animals were in accordance with recommendations of the Federation for Laboratory Animal Science Associations and approved by the local Institutional Animal Care and Use Committees. All possible efforts were made to minimize animal suffering and the number of animal used. Wistar rats (provided by the Sechenov Institute's Animal Facility) 16 days pregnant (10 animals in this study) were sacrificed by $CO_2$ inhalation.

### 2.2. Preparation and solutions

Cell cultures were prepared as described previously [4]. Fetuses (8–13) were removed from each pregnant female, and their cerebral cortices were isolated, enzymatically dissociated, and used to prepare primary neuronal cultures. Cells were used for experiments after 10–14 days in culture [4,28]. Neuronal cultures were perfused with indicated concentrations of drugs dissolved in the bathing solutions. The principal external bathing solution for patch clamp recordings and $Ca^{2+}$-imaging analysis on primary cultures of neurons from rat brain cortex consisted of 140 mM NaCl, 2.8 mM KCl, 2.0 mM $CaCl_2$, 1.0 mM $MgCl_2$, and 10 mM HEPES. The content of the external solution slightly varied depending on the purpose of the experiments. In experiments with *N*-methyl-D-aspartate (NMDA), $Mg^{2+}$ was omitted from the bathing solution, because it blocks the channels of NMDARs [29,30]. To trigger whole-cell currents and intracellular $Ca^{2+}$-responses 30 μM NMDA (30 μM glycine was present as a co-agonist of NMDARs [31]) or 30 μM KA were added to the external bathing solution. The pH of each external solution was adjusted to 7.4 with NaOH. Patch-clamp and $Ca^{2+}$-imaging experiments were performed at room temperature (20–23 °C).

### 2.3. Patch-clamp recording

Patch-clamp recordings were carried out on the stage of an inverted microscope Diaphot TMD (Nikon, Tokyo, Japan) with Hoffman modulation contrast optics. Patch pipettes (2–4 MΩ) were pulled from 1.5-mm (outer diameter) borosilicate standard wall capillaries with inner filament (Sutter Instrument Company, Novato, CA). Recordings were made using a MultiClamp 700B amplifier (Molecular Devices, Sunnyvale, CA). Whole-cell currents were recorded at membrane voltage of −70 mV during bath perfusion of 30 μM NMDA + 30 μM glycine or 30 μM KA or their fast application using a multibarrel perfusion system. Recordings of integral cellular currents were done by using whole-cell configurations of the patch-clamp technique. Continuous recordings were low-pass filtered at 400 Hz and digitized at 20 kHz with Digi-Data1440A and pClamp 10 software (Molecular Devices). In these experiments, pipettes were filled with a solution containing 9 mM NaCl, 17.5 mM KCl, 121.5 mM K-gluconate, 1 mM $MgSO_4$,10 mM HEPES, 0.2 mM EGTA, 2 mM MgATP, and 0.5 mM NaGTP [28].

### 2.4. Loading of $Ca^{2+}$-indicators and $Ca^{2+}$ imaging

Cells were loaded with Fluo-3 AM (4 μM), or Fura-2 AM (10 μM) by using conventional protocols, recommended by the manufacturer. In brief, neuronal cultures were incubated with the AM esters, and 0.02% Pluronic F-127 was added to the external solution for 45 min in the dark at room temperature. Then, the AM esters were washed out, and cells were incubated in the external solution for another 30 min in the dark. For Fluo-3 experiments, coverslips with loaded cultures were placed in the perfusion chamber that was mounted on the stage of a Leica TCS SP5 MF inverted microscope (Leica Microsystems, Inc., Bannockburn, IL). Fluorescence was activated with 488-nm laser light and emission was measured within the wavelength range from 500 to 560 nm. Some areas of neuronal culture contained glia, forming a thin flat layer subjacent to neuronal bodies bulging out above. To exclude glia from images we set confocal optical section (for 63× objective the thickness of optical section was 0.4 μm) to cross neuronal bodies only. Transmitted light images were also captured to verify the correct position of focal plane using morphological criteria. Images were captured every minute during 60-min experiments. For Fura-2 the perfusion chamber with neuronal cultures were mounted on the stage of a Nikon TMS inverted epifluorescence microscope (Nikon, Tokyo, Japan) equipped with a 300-W xenon lamp (Intracellular Imaging Inc., Cincinnati, OH) and 30× dry objective. Cells were visualized with a high-resolution digital black/white charge-coupled device camera Cohu 4910 (Cohu Electronics, Poway, CA), and $[Ca^{2+}]_i$ was estimated by the 340/380 ratio method, using a $K_d$ value of 315 nM for 23 °C. Imaging data were analyzed with InCytIm2 (Intracellular Imaging and Photometry System, Cincinnati, OH). All raw data were plotted using MS Excel. (Microsoft, Redmond, WA).

### 2.5. Drugs

All culture media were obtained from Biolot (Saint-Petersburg, RF). IEM-1460 was provided by Dr. V.E. Gmiro, the Institute of

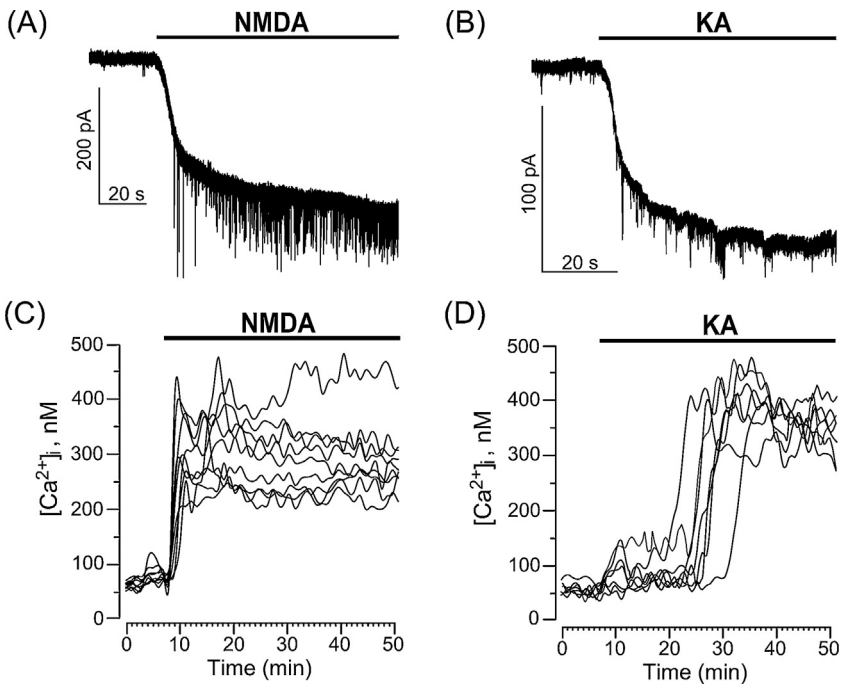


**Fig. 1.** Current and $Ca^{2+}$ responses of cultured cortical neurons to application of GluR agonists, NMDA and KA. (A) Representative whole-cell currents illustrating neuronal responses of cultured cortical neurons to application of 30 μM NMDA. (B) Representative whole-cell currents illustrating the response of cultured cortical neurons to application of 30 μM KA. The time of agonist application is indicated by the line above the traces. (C) Sustained $Ca^{2+}$-responses of neurons loaded with Fura-2 upon application of 30 μM NMDA (time of application shown by the line above the traces). Each trace represents the response of one neuron. Data from one experiment are plotted. Number of experiments $N = 4$. (D) $Ca^{2+}$-responses of neurons loaded with Fura-2 upon application of 30 μM KA (time of application shown by the line above the traces). Each trace represents the response of one neuron. Data from one experiment are plotted ($N = 4$).

Experimental Medicine RAMS (Saint-Petersburg, RF). Fura-2 AM was from Fluka (Buchs, Switzerland), Fluo-3 AM and Pluronic F-127 were from Molecular Probes (Carlsbad, CA). Ifenprodil was from Tocris (Bristol, UK). Other compounds were from Sigma–Aldrich (St. Louis, MO). Stock solutions of 10 mM NMDA, 10 mM glycine, 10 mM KA and 10 mM IEM-1460 dissolved in distilled water were stored frozen and thawed on the day of use. Stock solutions of 10 mM Fura-2 AM and 10 mM Fluo-3 AM dissolved in dimethylsulfoxide were stored frozen. Stock solutions of 1 mM ifenprodil dissolved in dimethylsulfoxide were stored refrigerated. All drugs were diluted in the external solution to the indicated concentrations before use.

## 3. Results

### 3.1. Comparison of time courses of inward currents and intracellular $Ca^{2+}$ responses caused by glutamate receptor agonists

We, first, performed experiments in which whole-cell currents were recorded during long-lasting 30 μM NMDA or 30 μM KA applications. Both agonists cause the generation of inward currents by neurons that rapidly rise to the maximum and remain at steady-state level as long as the agonists are present (Fig. 1A and B). For both NMDA and KA the rise time of inward currents corresponds to the time required for agonists to reach their final concentration in the chamber. Dynamics of intracellular $Ca^{2+}$ signals were measured using Fura-2 (Fig. 1C and D). Application of 30 μM NMDA to neurons (Fig. 1C) induced sustained intracellular $Ca^{2+}$ responses lasting as long as NMDA was present. It should be noted that all neurons responded to NMDA by increasing $[Ca^{2+}]_i$ and the dynamics of $[Ca^{2+}]_i$ rises corresponded well to the rise of inward current. In contrast neuronal $Ca^{2+}$ signals initiated by 30 μM KA developed much slower than the inward current. Application of 30 μM KA to neurons (Fig. 1D) induced intracellular $Ca^{2+}$ responses that differed in the dynamics of $[Ca^{2+}]_i$ elevations between cells. Some neurons responded in a similar way to those observed with NMDA experiments. However, most of the neurons demonstrated slow or delayed increases of $[Ca^{2+}]_i$ reaching maximum at 20–30 min of KA application (Fig. 1D). While the dynamics of intracellular $Ca^{2+}$ responses induced by NMDA and KA differed significantly, maximal $[Ca^{2+}]_i$ values obtained with both NMDA and KA were similar. On average somatic free $[Ca^{2+}]_i$ under control condition did not exceed 70 nM, whereas in the presence of NMDA or KA it could reach 0.5 μM and over in some cells (Fig. 1C and D).

### 3.2. Extracellular $Ca^{2+}$ is required to induce neuronal $Ca^{2+}$ responses by NMDA and KA

High $Ca^{2+}$ permeability of NMDAR channels is known to underlie $Ca^{2+}$ entry into neurons that determines the relatively synchronized generation of inward current and intracellular $Ca^{2+}$ response during NMDAR activation [14,15,32,33]. Removal of extracellular $Ca^{2+}$ before development of delayed calcium deregulation eliminates intracellular $Ca^{2+}$ signals even in the presence of glutamate, KA or NMDA [9,32,33]. The difference in dynamics of $[Ca^{2+}]_i$ elevations observed in the presence of NMDA and KA raises the question whether during AMPAR activation the source of $Ca^{2+}$ accumulating in the cytosol is from the extracellular medium or from the intracellular stores. Delayed development of $Ca^{2+}$ signals upon KA application (Fig. 1D) suggests that the $[Ca^{2+}]_i$ increase originates from $Ca^{2+}$ exit out of intracellular $Ca^{2+}$ stores (mitochondria, endoplasmic reticulum or Golgi apparatus). To address this question we performed experiments with Fluo-3 and Fura-2 in which NMDA or KA were applied in $Ca^{2+}$-free extracellular solutions and then after 30 min extracellular $Ca^{2+}$ was added. In $Ca^{2+}$-free external solution, application of 30 μM NMDA (Fig. 2A) or 30 μM KA (Fig. 2B) both did not cause the $[Ca^{2+}]_i$ increase, while the addition of $Ca^{2+}$ to the extracellular medium immediately triggered the $Ca^{2+}$ responses in both cases. Notably, NMDA-induced $Ca^{2+}$ responses are

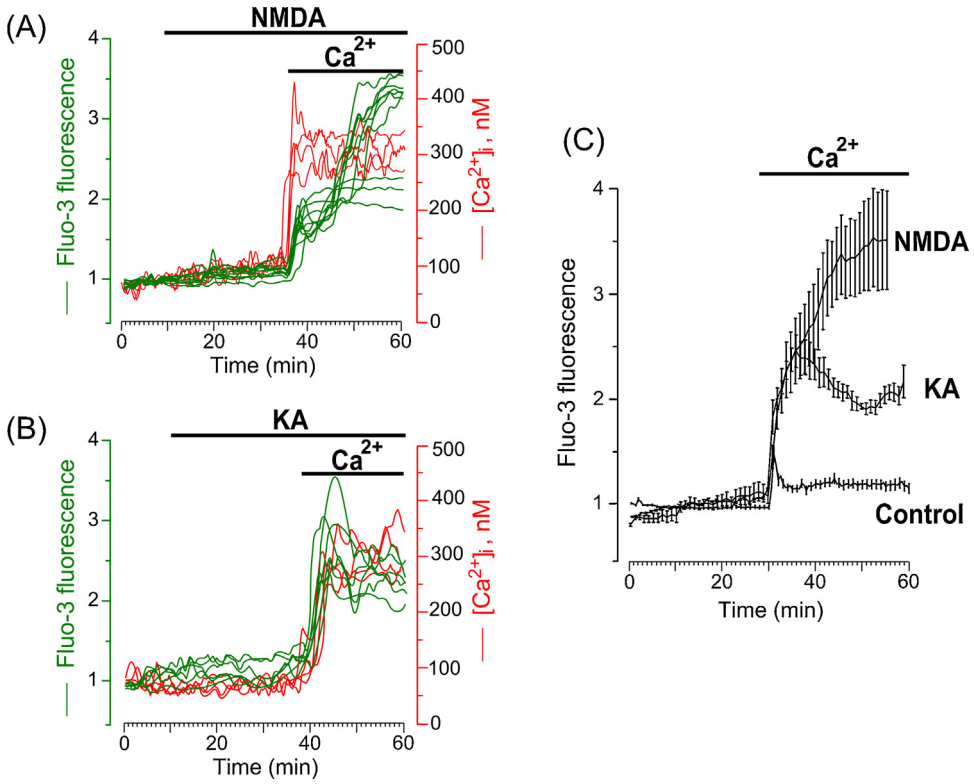


**Fig. 2.** Intracellular $Ca^{2+}$ signals induced by GluR agonists occur only when $Ca^{2+}$ is present in the external solution. (A) Time course of the $[Ca^{2+}]_i$ response after application of 30 μM NMDA in $Ca^{2+}$-free extracellular solution, followed by the addition of 2 mM $Ca^{2+}$ to the extracellular solution in the continued presence of 30 μM NMDA (the application episodes are marked with lines above the traces). Neurons were loaded with Fluo-3 (left ordinate, relative fluorescence intensity, green lines) and Fura-2 (right ordinate, $[Ca^{2+}]_i$, red lines). Each trace represents the response of one neuron. Data from two experiments (one with Fluo-3 and one with Fura-2) are plotted. Four ($N = 4$) experiments for each $Ca^{2+}$ indicator were performed. (B) Time course of the $[Ca^{2+}]_i$ response after application of 30 μM KA in $Ca^{2+}$-free extracellular solution, followed by the addition of 2 mM $Ca^{2+}$ to the extracellular solution in the continued presence of 30 μM KA (the application episodes are marked with lines above the traces). Neurons were loaded with Fluo-3 (left ordinate, relative fluorescence intensity, green lines) and Fura-2 (right ordinate, $[Ca^{2+}]_i$, red lines). Each trace represents the response of one neuron. Data from two experiments (one with Fluo-3 and one with Fura-2) are plotted. Four ($N = 4$) experiments for each $Ca^{2+}$ indicator were performed. (C) Comparison of average time courses of the $[Ca^{2+}]_i$ responses obtained in experiments with NMDA ($N = 3$, total number of analyzed neurons is 40), KA ($N = 4$, total number of analyzed neurons is 48) and in the absence of agonists (control, $N = 4$, total number of analyzed neurons is 83) upon an addition of 2 mM $Ca^{2+}$ to the $Ca^{2+}$-free extracellular solution. Mean values ± s.e. are plotted.

characterized by a fast development of delayed calcium deregulation (Fig. 2A) and KA-induced $Ca^{2+}$ responses are characterized by a rapid $[Ca^{2+}]_i$ increase (Fig. 2B). Averaged data from experiments with Fluo-3 in which 2 mM $Ca^{2+}$ was added to the external $Ca^{2+}$-free solution in the presence of NMDA or KA and in the absence of agonists are illustrated in Fig. 2C. Application of $Ca^{2+}$ in the absence of both agonists induced a small transient $[Ca^{2+}]_i$ increase that declined to the steady state level. Application of $Ca^{2+}$ in the presence of either agonist caused $[Ca^{2+}]_i$ increases that differed significantly from those obtained in their absence. Obviously, NMDA induced much greater $Ca^{2+}$ overload, than KA (Fig. 2C). These experiments demonstrate that, as for the NMDARs, $Ca^{2+}$ entry from the extracellular solution through transmembrane channels is required for the $[Ca^{2+}]_i$ increase when AMPARs are activated.

### 3.3. NMDARs of GluN1/GluN2B composition are mainly expressed in rat cortical neurons in primary cultures

To study the possible subunit composition of NMDARs expressed in rat cortical neurons of primary cultures we used ifenprodil, an allosteric inhibitor, that selectively binds to the extracellular domain of the GluN2B subunit and decreases the open probability of NMDARs containing GluN2B [1,25,26]. When applied during the $Ca^{2+}$-responses induced by NMDA, 10 μM ifenprodil considerably decreased $[Ca^{2+}]_i$ to about 10–30% of maximal values (Fig. 3A). When 10 μM ifenprodil was applied at the beginning of application simultaneously with NMDA, neurons generated weak $Ca^{2+}$-responses that were enhanced dramatically during ifenprodil washout (Fig. 3B). Experiments of both protocols clearly demonstrate that the majority of rat cortical neurons growing in culture express NMDARs comprised of GluN1/GluN2B receptors. This conclusion agrees well with a previous study examining mRNA levels in cortical neuronal cultures [34].

### 3.4. Expression of different AMPARs accounts for dynamics diversity of $Ca^{2+}$-responses to KA

Permeability of AMPAR channels to $Ca^{2+}$ and the effectiveness of their open-channel block by pharmacological agents are determined by the presence of the GluA2-subunit in their structure [1,21,22]. GluA2-lacking AMPARs have high $Ca^{2+}$ permeability and can be effectively blocked. For example, the $ED_{50}$ of the channel block of GluA2-lacking AMPARs with IEM-1460 is 1.6 μM [22], whereas this value for GluA2-containing AMPARs and NMDARs is over two orders of magnitude greater [22,27]. Because extracellular $Ca^{2+}$ is required to generate the intracellular $Ca^{2+}$-responses to KA (Fig. 2B), we used IEM-1460, a selective open-channel blocker of GluA2-lacking AMPARs, to study how $Ca^{2+}$-permeable AMPARs determine the dynamics of the KA-induced $[Ca^{2+}]_i$ increase. In these experiments 30 μM KA and 3 μM IEM-1460 were applied simultaneously to primary neuronal cultures loaded with Fluo-3. After 30 min, IEM-1460 was washed out (Fig. 4A). Images were

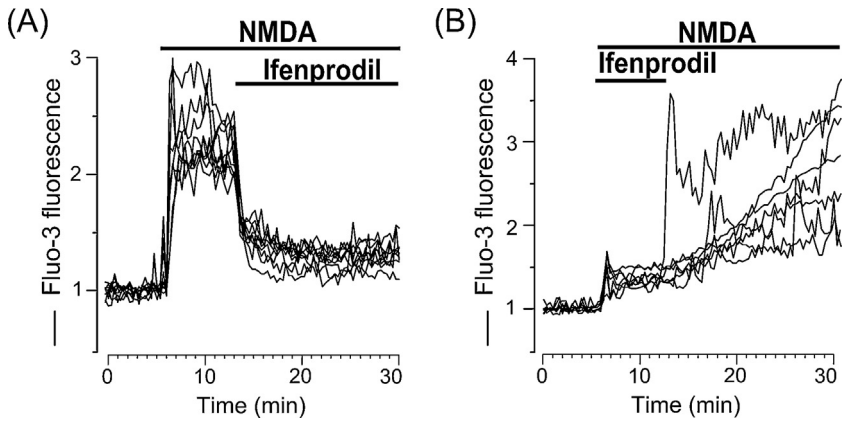


**Fig. 3.** Ifenprodil, a GluN2B selective antagonist of NMDARs, inhibits intracellular $Ca^{2+}$ responses induced by NMDA. (A) $Ca^{2+}$ responses measured upon application of 30 μM NMDA following by the addition 10 μM ifenprodil (the application episodes are marked with lines above the traces). Neurons were loaded with Fluo-3 (ordinate, relative fluorescence intensity). Each trace represents the response of one neuron. (B) $Ca^{2+}$ responses measured upon application of 30 μM NMDA with 10 μM ifenprodil following by ifenprodil washout (the application episodes are marked with lines above the traces). Neurons were loaded with Fluo-3 (ordinate, relative fluorescence intensity). Each trace represents the response of one neuron. Four experiments were performed.

captured every min. Representative images corresponding to the different stages of the experiments are shown in Fig. 4B. Based upon the type of intracellular $Ca^{2+}$-responses, these experiments revealed three approximately equal groups of cortical neurons (Fig. 4A). One group of neurons responded to combined application of IEM-1460 and KA with an increase in $[Ca^{2+}]_i$ accompanied by $Ca^{2+}$ oscillations and IEM-1460 washout was followed by a further rapid rise in $[Ca^{2+}]_i$ (Fig. 4A and B, red lines and circles). Another group of neurons also responded with an increase in $[Ca^{2+}]_i$ accompanied by $Ca^{2+}$ oscillations, but washout of IEM-1460 had no influence on the intracellular $[Ca^{2+}]_i$ signal (Fig. 4A and B, blue lines and circles). The last group of neurons did not exhibit any increase in $[Ca^{2+}]_i$ upon combined application of IEM-1460 and KA, but washout of IEM-1460 in the continued presence of KA caused a substantial elevation in $[Ca^{2+}]_i$ (Fig. 4A and B, green lines and circles). These data could be interpreted to suggest that the neurons express AMPARs of different subunit compositions. For instance, if neurons express the GluA2-containing AMPARs, IEM-1460 should not block their channels and as a consequence should not affect the intracellular $Ca^{2+}$-responses. In contrast IEM-1460 should block both the channel conductance and the intracellular $Ca^{2+}$ responses of neurons expressing GluA2-lacking AMPARs.

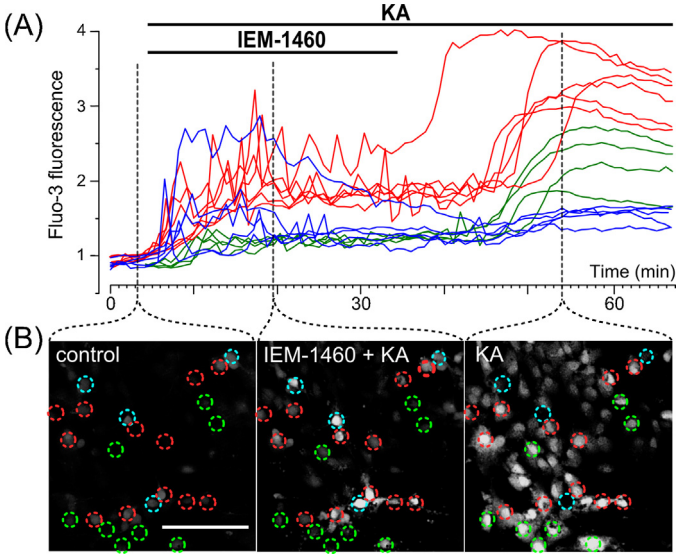


**Fig. 4.** Application of KA and IEM-1460, a subunit specific open channel blocker of AMPARs reveals three different types of intracellular $Ca^{2+}$ responses in cultured cortical neurons. (A) $Ca^{2+}$ responses upon application of 30 μM KA with 3 μM IEM-1460 followed by IEM-1460 washout (the application episodes are marked with lines above the traces). Neurons were loaded with Fluo-3 (ordinate, relative fluorescence intensity). Each trace represents the response of one neuron. Three ($N = 3$) experiments were performed. (B) Fluorescent images taken at different stages (indicated by dashed lines) of the experiment illustrated in (A). $Ca^{2+}$ responses of neurons marked by circles are plotted in panel A. Red, blue and green traces (in A) were obtained from neurons marked by circles of the same color. Scale bar is 100 μm and valid for all images. Detailed description and interpretation of these data are presented in Sections 3.4 and 4.4.

To further verify this suggestion we studied the inhibition by 3 μM or 10 μM IEM-1460 of whole-cell inward currents induced in neurons by 30 μM KA. The degree of block by IEM-1460 of KA induced currents differed dramatically between neurons (Fig. 5). In some neurons, 10 μM IEM-1460 had little or no effect on currents (Fig. 5A and B). Other neurons exhibited a strong degree of current block by 10 μM (Fig. 5C) or 3 μM (Fig. 5D) IEM-1460, revealing that these particular neurons express the GluA2-lacking AMPARs.

Thus, the agreement between the IEM-1460 data from patch-clamp electrophysiological and $Ca^{2+}$-imaging experiments allows us to conclude that the variability in the time course of the increase of $[Ca^{2+}]_i$ induced by KA is probably determined by different mechanisms of $Ca^{2+}$ entry and reflects the heterogeneity of the neuronal population in primary cultures from rat brain cortex with respect to expression of $Ca^{2+}$-permeable and -impermeable AMPARs.

### 3.5. Neuroprotective effect of subnanomolar ouabain

Experiments described above strikingly demonstrated that open-channel blockers are not effective tools to prevent KA-induced neurodegeneration, since they only block the channels of AMPARs in one third or even less cortical neurons. It has been demonstrated recently that subnanomolar concentrations of ouabain, a specific ligand of the Na/K-ATPase cardiac glycoside binding site, prevent the development of NMDA-induced $Ca^{2+}$ overload and protect cortical neurons against excitotoxicity [4]. To search for a pharmacological tool to minimize KA-induced neurodegeneration, we studied the effects of 1 nM ouabain on neuronal $Ca^{2+}$ overload caused by this glutamate agonist which is the most toxic for different types of neurons [18–20].

When 30 μM KA and 1 nM ouabain were applied to neurons simultaneously, the initial small increase of $[Ca^{2+}]_i$ was not followed by delayed intracellular $Ca^{2+}$ accumulation (Fig. 6A). Average data obtained with KA in the absence and presence of ouabain are compared in Fig. 6B. The results shown in Fig. 6B

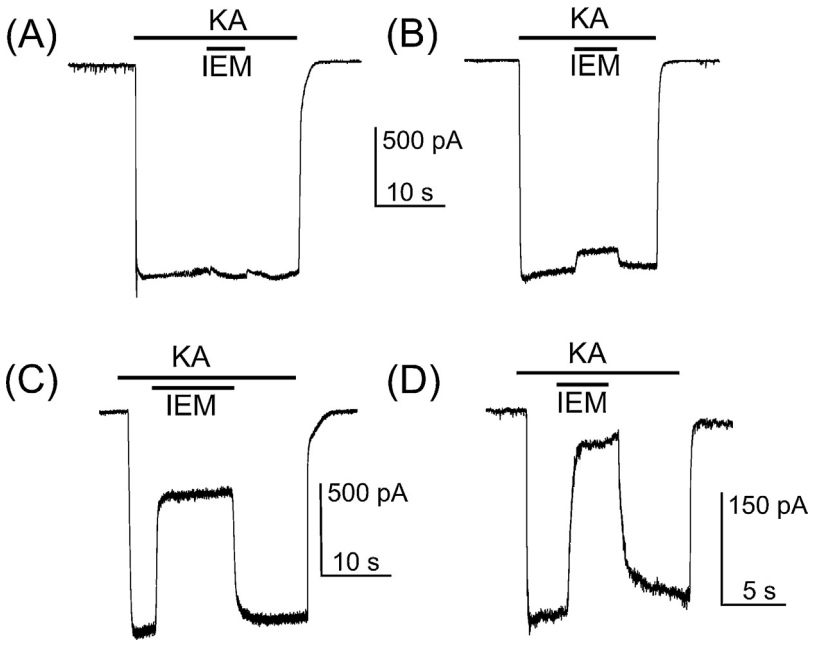


**Fig. 5.** Inhibition by IEM-1460 of whole-cell currents induced in neurons by 30 μM KA. (A) KA-induced current recorded from a neuron which is insensitive to 10 μM IEM-1460. (B) KA-induced current recorded from a neuron which is weakly blocked (8% of current is blocked) by 10 μM IEM-1460. (C) KA-induced current recorded from a neuron which is moderately blocked by IEM-1460. 60% of current is blocked by 10 μM IEM-1460. (D) KA-induced current recorded from a neuron which is strongly blocked by IEM-1460. 85% of current is blocked by 3 μM IEM-1460. The protocols of drug applications are shown above the current traces. The number of tested neurons is 24.

demonstrate that a subnanomalar concentration of ouabain, which does not affect enzymatic activity of the Na/K-ATPase [4], does prevent KA-induced neuronal $Ca^{2+}$ overload. Moreover, the $Ca^{2+}$ overload was prevented in the vast majority of neurons (Fig. 6A) suggesting that 1 nM ouabain protects neurons against KA-induced excitotoxicity independently from the mechanism of $Ca^{2+}$ entry in neurons. Therefore, subnanomolar concentrations of ouabain may be a great means of antagonizing KA-induced neurodegeneration.

## 4. Discussion

Open-channel block is a functionally important mechanism that regulates activity of many channels. Polyamine sensitive receptors and channels are widely represented in CNS playing a key role in neuronal and glial cell behavior and survival. Among them are highly (Kir2.1 [35]) and weakly (Kir4.1 [36]) sensitive potassium channels and glutamate receptors [37,38]. Endogenous polyamines are polycations that do not demonstrate selectivity between such receptors and channels [37], however recent advances in creating novel blockers of AMPA receptor channels allow us to use IEM1460, an adamantane based polycation which preferentially blocks GluA2-lacking AMPARs [21,22,27]. We found that agonist induced calcium accumulation in cortical neurons depends strongly on functional expression of glutamate receptor subunits and the results initiate the following discussion.

### 4.1. Possible importance of KA receptors for inward currents and neuronal $Ca^{2+}$-responses evoked by 30 μM KA

Normal synaptic functions of glutamate and neurodegeneration as a consequence of glutamate excitotoxicity are both mediated by activation of the same ionotropic GluRs. At central excitatory synapses, NMDARs colocalize with AMPARs to form the functional synaptic unit, such that presynaptically released glutamate typically activates both NMDARs and AMPARs [1]. In many brain structures, KA receptors [39] also play a role in presynaptic modulation of transmitter release and generation of EPSCs [40]. In cortex, KA receptors are expressed mainly in late embryonic and

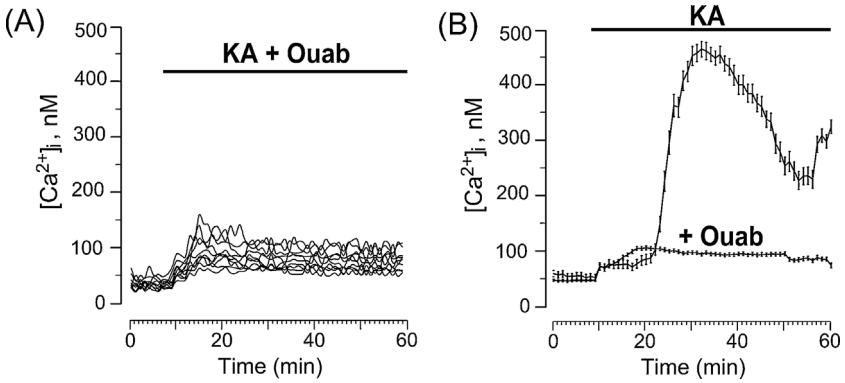


**Fig. 6.** Ouabain at 1 nM prevents $Ca^{2+}$ overload of neurons induced by KA. (A) $Ca^{2+}$ responses measured upon simultaneous application of 30 μM KA and 1 nM ouabain. Each trace represents the response of one neuron. Data from one experiment are plotted. (B) Comparison of average time course of the $[Ca^{2+}]_i$ responses obtained in experiments with 30 μM KA ($N = 3$, total number of analyzed neurons is 48) and 30 μM KA + 1 nM ouabain ($N = 3$, total number of analyzed neurons is 139). Mean values ± s.e. are plotted.

early postnatal states [41] and like AMPAR and NMDAR subunit expression are under developmental and regional control during the early postnatal life. To induce intracellular $Ca^{2+}$-responses in our experiments, we used KA which is not entirely selective for only KA receptors and activates AMPARs to produce large sustained currents [18,19]. In contrast to AMPARs, which are not desensitized by KA [18,19], KA receptors have high affinity to KA (about 1 μM) and have a rather fast rate of desensitization [42–44]. Under these particular conditions, even if KA receptors are still expressed in cultured neurons of 10–14 DIV, it seems unlikely that they may contribute to inward currents (Figs. 1B and 5) and neuronal $Ca^{2+}$-responses (Figs. 1D and 4) caused by 30 μM KA application.

### 4.2. Requirement of $Ca^{2+}$ presence in the extracellular media

The importance of NMDARs and AMPARs for excitotoxicity is obvious. The prolonged action of NMDA and KA, synthetic selective agonists of particular receptor types [1] which can not be utilized by neurons or glial cells, lead to neuronal death via necrosis or apoptosis [2–5]. According to the ratio of necrotic and apoptotic neurons, KA-induced neurotoxicity is more pronounced than NMDA-induced neurotoxicity [4]. During prolonged NMDA or KA exposure, neurons generate an intracellular $Ca^{2+}$ signal with subsequent delayed calcium deregulation [9] that reflects the $Ca^{2+}$ released from intracellular $Ca^{2+}$ stores. The dynamics of $[Ca^{2+}]_i$ increases elicited by NMDA and KA differ notably (Fig. 1C and D). While the $[Ca^{2+}]_i$ increase evoked by NMDA has a time course similar to the NMDA-induced inward current and rapidly reaches steady-state in the vast majority of neurons (Fig. 1A and C), the time course of the $[Ca^{2+}]_i$ increase evoked by KA differs between neurons and its development is delayed up to 20–30 min in many cells (Fig. 1C and D) if compared with corresponding KA-induced inward current (Fig. 1B and D). This delayed rise of $[Ca^{2+}]_i$ suggests that in the case of KA we observed delayed calcium deregulation, and the main source of free cytosolic $Ca^{2+}$ is due to release from mitochondria and other intracellular $Ca^{2+}$ stores.

To address this point we performed experiments, in which NMDA and KA were applied in $Ca^{2+}$-free external physiological solution. After 30 min of agonist exposure $Ca^{2+}$ was added to the extracellular media. For both agonists, there was no increase in $[Ca^{2+}]_i$ in the absence of $Ca^{2+}$ in the extracellular media and the addition of $Ca^{2+}$ triggered $Ca^{2+}$ responses for KA as well as for NMDA (Fig. 2). This observation suggests that for both agonists the source of $Ca^{2+}$ accumulating in the cytoplasm is from the extracellular media. Whereas the pathway of $Ca^{2+}$ entry in the case of NMDARs is clear, because NMDARs are highly $Ca^{2+}$ permeable [13–15], the variability of the dynamics of $[Ca^{2+}]_i$ increases in the case of AMPARs suggests the existence of more complex and unclear processes of $Ca^{2+}$ transfer through the plasma membrane.

### 4.3. NMDARs subunit compositions in cultured rat cortical neurons

NMDARs are thought to be heterotetramers comprised of two GluN1 subunits and two GluN2 (represented by GluN2A, 2B, 2C and 2D) or GluN3 subunits [1,45]. NMDAR subunit expression is under developmental and regional control. NMDARs differ in their kinetics of activation, conductance, open channel block by $Mg^{2+}$ and $Ca^{2+}$-permeability [1]. In this respect GluN1/GluN2A and GluN1/GluN2B receptors have similar characteristics. To study the possible NMDAR subunit composition in cultured rat cortical neurons which are involved in the generation of inward currents and intracellular $Ca^{2+}$ signals, we used the subunit-selective NMDA receptor antagonist, ifenprodil [25,26]. This compound is a noncompetitive, voltage-independent partial antagonist (maximal inhibition ~90%) of GluN2B-containing NMDARs. Ifenprodil inhibits GluN2B-containing receptors with high affinity ($IC_{50}$ of ~150 nM) and is 200 to 400-fold more potent for GluN1/GluN2B receptors than for others [25,26]. In our experiments ifenprodil, when applied after NMDA (Fig. 3A) or with NMDA (Fig. 3B), partially inhibits intracellular $Ca^{2+}$-responses to 10–30% of maximal values. Even using saturating concentrations of ifenprodil, the remaining $Ca^{2+}$ response after reaching the steady state is substantially above 10% of the maximal $[Ca^{2+}]_i$. This suggests that activation of GluN1/GluN2B receptor channels mainly determines the $Ca^{2+}$ transfer through the plasma membrane in these neurons. However, due to incomplete inhibition one may not exclude some contribution of other NMDARs. Taking into account that the existence of GluN2C and GluN2D has never been reported in primary rat cortical cultures, most probably these are the GluN1/GluN2A receptors. This conclusion is consistent with previous observations that cultured rat cortical neurons express mRNA encoding the GluN1, GluN2A and GluN2B subunits of NMDARs [34].

### 4.4. AMPARs are expressed in cortical neurons in vitro

In general excitatory synaptic transmission in the CNS of vertebrates is mediated by heteromeric AMPARs assembled from differing combinations of the four subunits, GluA1 to GluA4. The presence or absence of GluA2 is a critical determinant of AMPAR function and dictates $Ca^{2+}$-permeability and the ability of their channels to be blocked by endogenous modulators and organic channel blockers [1]. An absence of GluA2 renders the channel pore permeable to $Ca^{2+}$ [21,38] and sensitive to extra- and intracellular polyamine block, endowing AMPARs with an inwardly rectifying current-voltage relationship [38,46,47] and a novel postsynaptic mechanism of short-term plasticity involving the use-dependent unblock of polyamines [48,49].

An additional pathway for the $Ca^{2+}$ entry in neurons other than NMDARs, therefore, can be provided by the $Ca^{2+}$-permeable AMPARs. Inherent coupling between the $Ca^{2+}$ permeability and the effectiveness of AMPAR channel block by organic compounds [22,50] allows us to distinguish pharmacologically GluA2-lacking AMPARs using subunit specific open channel blockers. Originally, it was shown that the polyamine toxins, purified from spider venoms, $argiotoxin_{636}$ or argiopine [51–54], block the channels of GluA2-lacking AMPARs, while the channel block of GluA2-containing AMPARs is weak [50]. The same principle applies for IEM-1460 [22]. With an $ED_{50}$ value of 1.6 μM, this compound blocks the channels of $Ca^{2+}$-permeable GluA2-lacking AMPARs [22]. To block channels of NMDARs and $Ca^{2+}$-impermeable GluA2-containing AMPARs at least 10 to 100-fold larger concentrations of IEM-1460 are needed [27,55].

In our experiments using KA and IEM-1460, we observed three types of $Ca^{2+}$-signal behavior which probably reflect the existence of several groups of neurons expressing different native AMPARs (Fig. 4). The variability found between neurons in the degree of block by IEM-1460 of whole-cell currents induced by KA (Fig. 5) is also consistent with this idea. Possible interpretations of the data are illustrated in Fig. 7. The first type of $Ca^{2+}$-response (green traces in Fig. 4A) could correspond to neurons which express $Ca^{2+}$-permeable GluA2-lacking AMPARs. These channels are blocked in the presence of 3 μM IEM-1460 and 30 μM KA preventing either $Ca^{2+}$ entry into the neurons and depolarization of neurons (Fig. 7A and B, upper part of schematic). Washout of IEM-1460 causes channel unblock resulting in an elevation of $[Ca^{2+}]_i$.

A second type $Ca^{2+}$-signal behavior (blue traces in Fig. 4A) can be observed when neurons express the $Ca^{2+}$-impermeable GluA2-containing AMPARs (Fig. 7A and B middle part of schematic). In this situation, IEM-1460 would not be able to block the receptor channels and depolarization induced by KA would cause an activation of voltage-dependent $Ca^{2+}$-channels. As a result oscillations of the

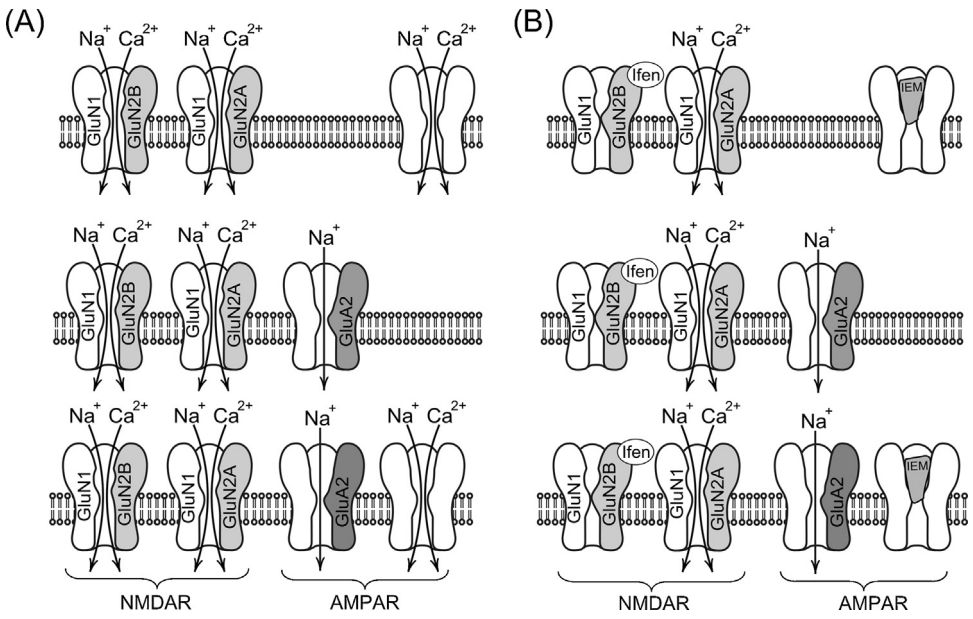


**Fig. 7.** Schematic of the data interpretation. (A) In the presence of GluR agonists, extracellular $Ca^{2+}$ can enter neurons through the channels of NMDARs and $Ca^{2+}$-permeable channels of GluA2-lacking AMPARs. (B) Ifenprodil by inhibiting GluN1/GluN2B prevents $Ca^{2+}$ entry through these particular NMDARs. $Ca^{2+}$, therefore, may enter the cytoplasm through the channels of GluN1/GluN2A only. IEM-1460 by blocking the $Ca^{2+}$ permeable channels of AMPARs abolishes $Ca^{2+}$ signals in neurons expressing GluA2-lacking AMPARs. Detailed description of data interpretation is presented in Section 4.4.

intracellular $Ca^{2+}$-signal are observed in the presence of IEM-1460, whereas its removal does not induce any additional changes in the $Ca^{2+}$-signal.

The third $Ca^{2+}$-response represents a hybrid of the two previously described responses (Fig. 4A, red traces). If neurons express both GluA2-lacking and GluR2-containing AMPARs, then both the $Ca^{2+}$-oscillations in the presence of IEM-1460 and the $[Ca^{2+}]_i$ rise upon washout of IEM-1460 could be observed (Fig. 7, lower part of schematic). This explanation would be slightly modified if there is some residual contribution from the rapidly desensitizing KA receptors. In this case KARs, whose channels are permeable to $Ca^{2+}$ and can be blocked by argiotoxin$_{636}$ [56], could be theoretically involved in responses indicated by green and red traces in Fig. 4A. However, because KARs are rapidly desensitized [42–44], if they participated in these responses we would expect to observe a decrease in current in Figs. 1B and 5 in response of KA application. This is not the case and therefore KARs most likely do not participate in $[Ca^{2+}]_i$ signals during long lasting KA application (Figs. 1B, D and 5A–D). In addition, since the key subunit GluA2, which governs $Ca^{2+}$ channel permeability and the channel block, belongs to the AMPAR type [1], we have omitted KARs from our scheme.

Principle neurons in forebrain are known to express AMPARs of different subunit composition. Expression of all subunits is developmentally regulated, region and cell-type specific, and activity-dependent [57]. For example, it has been demonstrated using IEM-1460 that pyramidal neurons of hippocampus express GluA2-containing AMPARs but interneurons usually have AMPARs without GluA2 [22]. In addition sensorimotor polysynaptic EPSPs are blocked by argiopine, while sensorimotor monosynaptic EPSPs are resistant to this neurotoxin in frog motoneurons [58]. This suggests that different AMPARs are involved in mono- and polysynaptic excitatory inputs. This makes it possible to correlate the dynamics of the $Ca^{2+}$ responses to KA and the effects of subunit-specific channel blockers to morpho-functional types of neurons. If this is the case, then neurons which are resistant to the IEM-1460 action can be classified as principal cells, while neurons which reveal block of currents and KA evoked $Ca^{2+}$ signals by IEM-1460 may represent different types of interneurons. We can conclude, therefore, that neurons in primary cultures are not uniform and probably maintain their morphological and functional phenotypes of the adult brain cortex.

The functional diversity of neurons existing in the CNS and cortical neurons in culture makes open-channel blockers of AMPARs ineffective as neuroprotective agents against KA excitotoxicity. Here we demonstrate that 1 nM ouabain prevents the $Ca^{2+}$ overload induced by KA (Fig. 6) independently from the mechanism of $Ca^{2+}$ entry in neurons [4]. This makes ouabain at subnanomolar concentrations an effective tool to prevent KA-induced neurodegeneration [4]. The neuroprotective concentration of ouabain used in this study corresponds well to the endogenous ouabain levels which vary from 0.1 nM to 0.74 nM in rat blood plasma and cerebrospinal fluid [59]. Similar neuroprotective effects of low ouabain concentrations have been demonstrated in another neurodegeneration model when KA and ouabain were injected into the brain in vivo [60]. Currently, ouabain (strophanthin-G) and other cardiac glycosides are used at low doses (which do not suppress the Na/K-ATPase) to prevent development of kidney failure [61], heart ischemia [62], or neuronal apoptosis [4,60]. These observations provide evidence for the (patho)physiological relevance of endogenous ouabain [59] which probably works via multiple pathways involving many different receptors localized in the membrane, cytoplasm and nuclei linked to $Ca^{2+}$-dependent second messenger systems [4,59–64]. Thus, the data presented here demonstrate a functional role of the $Na^+/K^+$-ATPase in intracellular $Ca^{2+}$ homeostasis that might be governed by binding of endogenous ouabain or its analogs to a highly conserved cardiotonic/ouabain receptor site.

## Acknowledgments

The work was supported by the Russian Foundation for Basic Research (11-04-00397), the Russian Federation Ministry of Education and Science (Contract 8476 to Sechenov IEPhB RAS) and

The National Institutes of Health (NS065201, GM088019 and MD007583).

## References


[1] S.F. Traynelis, L.P. Wollmuth, C.J. McBain, et al., Glutamate receptor ion channels: structure, regulation and function, Pharmacological Reviews 62 (2010) 405–496.
[2] D.W. Choi, Excitotoxic cell death, Journal of Neurobiology 23 (1992) 1261–1276.
[3] J.W. Olney, Excitatory transmitter neurotoxicity, Neurobiology of Aging 15 (1994) 259–260.
[4] D.A. Sibarov, A.E. Bolshakov, P.A. Abushik, I.I. Krivoi, S.M. Antonov, $Na^+$, $K^+$-ATPase functionally interacts with the plasma membrane $Na^+$, $Ca^{2+}$-exchanger to prevent $Ca^{2+}$ overload and neuronal apoptosis in excitotoxic stress, Journal of Pharmacology and Experimental Therapeutics 343 (2012) 596–607.
[5] D.W. Choi, Glutamate neurotoxicity and diseases of the nervous system, Neuron 1 (1988) 623–634.
[6] B. Meldrum, Amino acids as dietary excitotoxins: a contribution to understanding neurodegenerative disorders, Brain Research 18 (1993) 293–314.
[7] S.A. Lipton, Ischemic cell death in brain neurons, Physiological Reviews 79 (1999) 1431–1537.
[8] C.G. Parsons, W. Danysz, G. Quack, Glutamate in CNS disorders as a target for drug development: an update, Drug News and Perspectives 11 (1998) 523–569.
[9] B. Khodorov, Glutamate-induced deregulation of calcium homeostasis and mitochondrial dysfunction in mammalian central neurons, Progress in Biophysics and Molecular biology 86 (2004) 279–351.
[10] S.M. Antonov, L.G. Magazanik, Intense nonquantal release of glutamate in an insect neuromuscular junction, Neuroscience Letters 93 (1988) 204–208.
[11] M. Szatkowski, B. Barbour, D. Attwell, Non-vesicular release of glutamate from glial cells by reversed electrogenic glutamate uptake, Nature 348 (1990) 443–446.
[12] D.J. Rossi, T. Oshima, D. Attwell, Glutamate release in sever brain ischemia is mainly by reversed uptake, Nature 403 (2000) 316–325.
[13] P. Ascher, L. Nowak, The role of divalent cations in the *N*-methyl-D-aspartate responses of mouse central neurones in culture, Journal of Physiology 399 (1988) 247–266.
[14] N. Burnashev, Z. Zhou, E. Neher, B. Sakmann, Fractional calcium currents through recombinant GluR channels of the NMDA, AMPA and kainite receptor subtypes, Journal of Physiology 485 (1995) 403–418.
[15] A.B. MacDermott, M.L. Mayer, G.L. Westbrook, S.J. Smith, J.L. Barker, NMDA-receptor activation increases cytoplasmic calcium concentration in cultured spinal cord neurons, Nature 321 (1986) 519–522.
[16] J.M. Dubinsky, S.M. Rothman, Intracellular calcium concentration during "chemical hypoxia" and excitotoxic neuronal injury, Journal of Neuroscience 11 (1991) 2545–2551.
[17] D.G. Nicholls, Mitochondrial dysfunction and glutamate excitotoxicity studied in primary neuronal cultures, Current Molecular Medicine 4 (2004) 149–177.
[18] N.I. Kiskin, O.A. Krishtal, A.Ya. Tsyndrenko, Excitatory amino acid receptors in hippocampal neurons: kainate fails to desensitize them, Neuroscience Letters 63 (1986) 225–230.
[19] D.K. Patneau, M.L. Mayer, Kinetic analysis of interactions between kainite and AMPA: evidence for activation of a single receptor in mouse hippocampal neurons, Neuron 6 (1991) 785–798.
[20] J. Garthwaite, G. Garthwaite, The mechanism of kainic acid neurotoxicity, Nature 305 (1983) 138–140.
[21] N. Burnashev, H. Monyer, P.H. Seeburg, B. Sakmann, Divalent ion permeability of AMPA receptor channels is dominated by the edited form of a single subunit, Neuron 8 (1992) 189–198.
[22] L.G. Magazanik, S.L. Buldakova, M.V. Samoilova, V.E. Gmiro, I.R. Mellor, P.N. Usherwood, Block of open channels of recombinant AMPA receptors and native AMPA/kainite receptors by adamantine derivatives, Journal of Physiology 505 (1997) 655–663.
[23] J. Grosskreutz, K. Haastert, M. Dewil, et al., Role of mitochondria in kainite-induced fast $Ca^{2+}$ transients in cultured spinal motor neurons, Cell Calcium 42 (2007) 59–69.
[24] N. Brunet, O. Tarabal, J.E. Esquerda, J. Caldero, Excitotoxic motoneuron degeneration induced by glutamate receptor agonists and mitochondrial toxins in organotypic cultures of chick embryo spinal cord, Journal of Comparative Neurology 516 (2009) 277–290.
[25] K. Williams, Ifenprodil discriminates subtypes of the *N*-methyl-D-aspartate receptor: selectivity and mechanisms at recombinant heteromeric receptors, Molecular Pharmacology 44 (1993) 851–859.
[26] E.R. Whittemore, V.I. Ilyin, R.M. Woodward, Antagonism of *N*-methyl-D-aspartate receptors by sigma sute ligands: potency, subtype-selectivity and mechanisms of inhibition, Journal of Pharmacology and Experimental Therapeutics 282 (1997) 326–338.
[27] S.M. Antonov, J.W. Johnson, N.Y. Lukomskaya, N.N. Potapyeva, V.E. Gmiro, L.G. Magazanik, Novel adamantane derivatives act as blockers of open ligand-gated channels and as anticonvulsants, Molecular Pharmacology 47 (1995) 558–567.
[28] E.B. Han, C.F. Stevens, Development regulates a switch between post- and presynaptic strengthening in response to activity deprivation, Proceedings of the National Academy of Sciences of the United States of America 106 (2009) 10817–10822.
[29] M.L. Mayer, G.L. Westbrook, P.B. Guthrie, Voltage-dependent block by $Mg^{2+}$ of NMDA responses in spinal cord neurons, Nature 309 (1984) 261–263.
[30] L. Nowak, P. Bregestovski, P. Ascher, A. Herbet, A. Prochiantz, Magnesium gates glutamate-activated channels in mouse central neurons, Nature 307 (1984) 462–465.
[31] J.W. Johnson, P. Ascher, Glycine potentiates the NMDA response in cultured mouse brain neurons, Nature 325 (1987) 529–531.
[32] A.V. Wabnitz, T.V. Kolesnikova, A.M. Surin, B.I. Khodorov, Y.E. Senilova, V.G. Pinelis, Delayed $Ca^{2+}$ deregulation in young cerebellar granule cells induced by overstimulation of glutamate receptors. Role of NMDA channels, Biological Membranes 23 (2006) 311–319.
[33] D. Bano, K.W. Young, C.J. Guerin, et al., Cleavage of the plasma membrane $Na^+/Ca^{2+}$ exchanger in excitotoxicity, Cell 120 (2005) 275–285.
[34] J. Zhong, S.L. Rassell, D.B. Pritchett, P.B. Molinoff, K. Williams, Expression of mRNA encoding subunits of the *N*-methyl-D-aspartate receptor in cultured cortical neurons, Molecular Pharmacology 45 (1994) 846–853.
[35] A.N. Lopatin, E.N. Makhina, C.G. Nichols, Potassium channel block by cytoplasmic polyamines as the mechanism of intrinsic rectification, Nature 372 (1994) 366–369.
[36] Y.V. Kucheryavykh, Y.M. Shuba, S.M. Antonov, et al., Complex rectification of Müller cell Kir currents, Glia 56 (2008) 775–790.
[37] K. Williams, Interactions of polyamines with ion channels, Biochemical Journal 325 (1997) 289–297.
[38] D.S. Koh, N. Burnashev, P. Jonas, Block of native $Ca^{2+}$-permeable AMPA receptors in rat brain by intracellular polyamines generates double rectification, Journal of Physiology 486 (1995) 305–312.
[39] J.E. Huettner, Kainate receptors and synaptic transmission, Progress in Neurobiology 70 (2003) 387–407.
[40] P.S. Pinheiro, C. Mulle, Presynaptic glutamate receptors: physiological function and mechanisms of action, Nature Reviews Neuroscience 9 (2008) 423–436.
[41] S. Bahn, B. Volk, W. Wisden, Kainate receptor gene expression in the developing rat brain, Journal of Neuroscience 14 (1994) 5525–5547.
[42] J. Lerma, A.V. Paternain, J.R. Naranjo, B. Mellstrom, Functional kainate-selective glutamate receptors in cultured hippocampal neurons, Proceedings of the National Academy of Sciences of the United States of America 90 (1993) 11688–11692.
[43] K.A. Jones, T.J. Wilding, J.E. Huettner, A.M. Costa, Desensitization of kainate receptors by kainate, glutamate and diastereomers of 4-methylglutamate, Neuropharmacology 36 (1997) 853–863.
[44] A.V. Paternain, A. Rodriguez-Moreno, A. Villarroel, J. Lerma, Activation and desensitization properties of native and recombinant kainate receptors, Neuropharmacology 37 (1998) 1249–1259.
[45] R.J. Wenthold, K. Prybylowski, S. Standley, N. Sans, R.S. Petralia, Trafficking of NMDA receptors, Annual Review of Pharmacology and Toxicology 43 (2003) 335–358.
[46] D. Bowie, M.L. Mayer, Inward rectification of both AMPA and kainite subtype glutamate receptors generated by polyamine-mediated ion channel block, Neuron 15 (1995) 453–462.
[47] V.A. Panchenko, C.R. Glasser, K.M. Partin, M.L. Mayer, Amino acid substitutions in the pore of rat glutamate receptors at sites influencing block by polyamines, Journal of Physiology 520 (1999) 337–357.
[48] A. Rozov, N. Burnashev, Polyamine-dependent facilitation of postsynaptic AMPA receptors counteracts paired-pulse depression, Nature 401 (1999) 594–598.
[49] J.T. Isaac, M. Ashby, C.J. McBain, The role of the GluR2 subunit in AMPA receptor function and synaptic plasticity, Neuron 54 (2007) 859–871.
[50] S. Herlitze, M. Raditsch, J.P. Ruppersberg, W. Jahn, H. Monyer, R. Schoepfer, V. Witzemann, Argiotoxin detects molecular differences in AMPA receptor channels, Neuron 10 (1996) 1131–1140.
[51] E.V. Grishin, T.M. Volkova, A.S. Arsen'ev, et al., Structural-functional characteristics of argiopine – the ion channel blockers from the spider Argiope lobata venom, Bioorganicheskaia Khimiia 12 (1986) 1121–1124.
[52] T. Budd, P. Clinton, A. Dell, et al., Isolation and characterization of glutamate receptor antagonists from venoms of orb-web spiders, Brain Research 448 (1988) 30–39.
[53] H. Jackson, P.N. Usherwood, Spider toxins as tools for dissecting elements of excitatory amino acid transmission, Trends in Neurosciences 11 (1988) 278–283.
[54] S.M. Antonov, J. Dudel, C. Franke, H. Hatt, Argiopine blocks glutamate-activated single-channel currents on crayfish muscles by two mechanisms, Journal of Physiology 419 (1989) 569–587.
[55] S.M. Antonov, V.E. Gmiro, J.W. Johnson, Binding sites for permeant ions in the channel of NMDA receptors and their effects on channel block, Nature Neuroscience 1 (1998) 451–461.
[56] R. Bähring, M.L. Mayer, An analysis of philanthotoxin block for recombinant rat GluR6(Q) glutamate receptor channels, Journal of Physiology 509 (1998) 635–650.
[57] M.C. Ashby, M.I. Daw, J.T.R. Isaac, AMPA receptors, in: R.W. Gereau, G.T. Swanson (Eds.), The Glutamate Receptors, Humana Press, Totowa, NJ, 2008, pp. 1–44.
[58] S.M. Antonov, N.I. Kalinina, G.G. Kurchavyj, L.G. Magazanik, O.V. Shupliakov, N.P. Vesselkin, Identification of two types of excitatory monosynaptic inputs in frog spinal motoneurons, Neuroscience Letters 109 (1990) 82–87.

[59] M. Dobretsov, J.R. Stimers, Neuronal function and alpha3 isoform of the Na/K-ATPase, Frontiers in Bioscience 10 (2005) 2373–2396.
[60] W.C. Golden, L.J. Martin, Low-dose ouabain protects against excitotoxic apoptosis and up-regulates nuclear BCL-2 in vivo, Neuroscience 137 (2006) 133–144.
[61] J. Li, G.R. Khodus, M. Kruusmägi, et al., Ouabain protects against adverse developmental programming of the kidney, Nature Communications 1 (2010) 1–7.
[62] P. Pasdois, C.L. Quinlan, A. Rissa, et al., Ouabain protects rat hearts against ischemia-reperfusion injury via pathway involving src kinase, mitoKATP, and ROS, American Journal of Physiology: Heart and Circulatory Physiology 292 (2007) H1470–H1478.
[63] I.I. Krivoi, T.M. Drabkina, V.V. Kravtsova, et al., On the functional interaction between nicotinic acetylcholine receptor and Na+, K+ -ATPase, Pflugers Archiv 452 (2006) 756–765.
[64] A.V. Chibalin, J.A. Heiny, B. Benziane, et al., Chronic nicotine modifies skeletal muscle Na, K-ATPase activity through its interaction with the nicotinic acetylcholine receptor and phospholemman, PLoS One 7 (2012) e33719.